J. Cent. South Univ. (2014) 21: 775−789
DOI: 10.1007/s11771-014-2001-9

Springer

Methodology for estimating probability of dynamical system's failure for concrete gravity dam

WANG Chao(王超), ZHANG She-rong(张社荣), SUN Bo(孙博), WANG Gao-hui(王高辉)

State Key Laboratory of Hydraulic Engineering Simulation and Safety (Tianjin University), Tianjin 300072, China

Abstract: Methodology for the reliability analysis of hydraulic gravity dam is the key technology in current hydropower construction. Reliability analysis for the dynamical dam safety should be divided into two phases: failure mode identification and the calculation of the failure probability. Both of them are studied based on the mathematical statistics and structure reliability theory considering two kinds of uncertainty characters (earthquake variability and material randomness). Firstly, failure mode identification method is established based on the dynamical limit state system and verified through example of Koyna Dam so that the statistical law of progressive failure process in dam body are revealed; Secondly, for the calculation of the failure probability, mathematical model and formula are established according to the characteristics of gravity dam, which include three levels, that is element failure, path failure and system failure. A case study is presented to show the practical application of theoretical method and results of these methods.

Key words: concrete gravity dam; dynamical system; failure mode identification; calculation of system failure probability; stochastic model

1 Introduction

The uncertainty of dynamic system of a concrete gravity dam mainly comes from two aspects. One is the earthquake variability; the other is the randomness of material. Variability of seismic load and anisotropism of concrete may lead to new failure modes for the concrete gravity dam under seismic loads. Consequently, methodology for estimating probability of the dynamical system's failure for concrete gravity dam should be studied for its random, progressive and complicated characters. Generally speaking, reliability analysis for the dynamical dam safety should be divided into two phases: failure mode identification and the calculation of the failure probability.

For the failure mode identification, there are many approaches, like network searching method, load increment method, branch-and-bound algorithm and so on. But the truth is that they don't work when meeting the mass concrete structures because it doesn't mean disabled when the damage only occurs on one section or some components. As a result, it brings difficulties to seek the dynamic failure modes for the mass concrete structures, like the concrete gravity dam.

Early studies usually made artificially assumed failure modes, based on the function of structural system of gravity dam. According to the stress analysis by 3-D nonlinear FEM, ZHU et al [1] assumed anti-sliding failure mode of gravity dam. FAN et al [2] assumed many modes of dam failure, foundation failure, sliding failure and gate lifting failure. With the improvement of research, XU et al [3] assumed failure mode oriented by the composite limit state function and found out corresponding failure paths. HONG et al [4] introduced all phases' mechanical properties of concrete, established microscopic probability model of concrete, put forward the analysis method of structure failure mode, based on the numerical simulation of microscopic in homogeneity model, and got the failure modes of gravity dam dynamic system.

For the calculation of the failure probability, it is always the hot issue in the field of water conservancy and hydropower science. Successful attempts on the calculation of gravity dam dynamic reliability in time domain have been carried out by WU and ZHUO [5]. Based on the assumed mode of gravity dam function failure, FAN et al [2] calculated two opposite extreme situations of perfect correlation and perfect un-correlation. JIA and ZHANG [6] studied the safety and reliability of RCC gravity dam with the method of stochastic finite element under the situation of exiting of horizontal weak bedding. WU et al [7] used Lagrange multiplier rule, turned solving design checking point

Foundation item: Projects(51021004, 51379141) supported by the Foundation for Innovative Research Groups of the National Natural Science Foundation of China
Received date: 2013−01−10; **Accepted date:** 2013−11−27
Corresponding author: WANG Chao, PhD; Tel: +86−22−27892185; E-mail: wangchaosg@tju.edu.cn

nonlinear constrained optimization problems with the restraint of response surface into solving linear equations response surfaces. XU et al [8] established a gravity dam failure path reliability calculation method on the process of non-stationary ground motion. Besides, based on Bayes formula and Cauchy-Schwarz inequality, XU et al [3] calculated the reliability of whole dam system with the method of derivating the upper limit of failure probability when the dam fails in certain failure mode.

But there are still many problems need to be solved for reliability analysis of gravity dam under the effects of earthquake. On one hand, the search method of failure path needs to be improved. Based on the finite element method, from the view of probability, searching the order of failure and failure route is a searching process for all elements. By using this kind of method, it would be a huge calculation. It's not suitable for engineering applications. On the other hand, the failure mode is relatively simple at present, and it is focused on reliability for local tensile. So, it needs further research with multiple failure modes.

2 Proposed methodology

Reliability techniques have been applied frequently to other kinds of problems in the geotechnical field, such as slope stability, which has received considerable attentions [9−13].

Generally, dam safety of the dynamical system based on reliability analysis methodology demands two parts, failure mode identification and the quantification of the failure probability of the system, so that the methodology described herein is divided in two phases and reflected in Fig. 1. It is considered that its application to any other type of dam and for any other failure modes can be carried out rather straightforwardly due to its generic formulation.

2.1 Phases 1: Methodology for failure mode identification

Failure mode identification of the dynamical dam system is the foundation of the reliability analysis. The starting point, **Step 1**, should always be the existence of a stochastic model fully defined and completed for the concrete dam; **Step 2** is the random search for the potential failure modes by controlled numerical simulation, which considers the variability of the variables (loads and parameters), based on the limit state dynamical system of the dam rather than the probability evaluation system, which costs much and is hard to reflect the mechanical meaning; **Step 3** is the failure mode generalization and identification based on the statistical characteristics from the random numerical simulations, which would be proved through Koyna Dam example in Section 3.

2.1.1 **Step 1**: Defining stochastic model

The stochastic model fully defined and completed for the concrete dam should include the definition of the loading scenarios and analysis of variables (loads and parameters) that appear in the problem. The variables are classified whether as determined variables, whose values are known with very little uncertainty, or as random variables, whose values are not known with precision and their knowledge is, therefore, reliant on uncertainty.

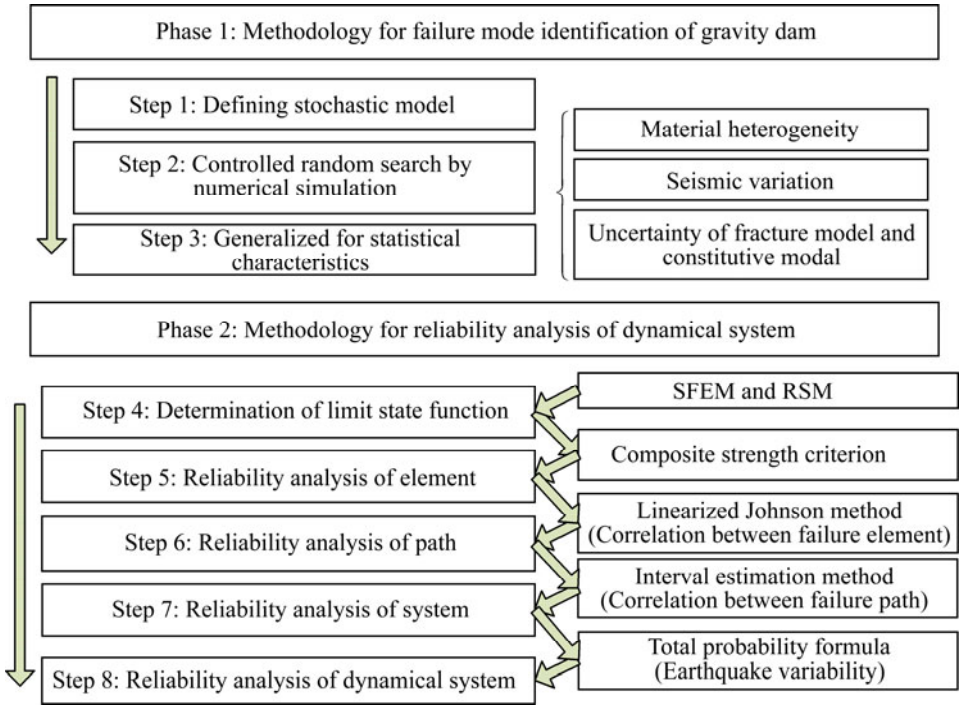

Fig. 1 Flow chart for estimation of probability of failure of concrete dams

For the variables considered as random, it is necessary to find out which are their probability distribution functions. In order to assess the probability distributions of the variables, results of research, tests and all the information available from the assessment of the dam should be taken into account [14].

2.1.2 **Step 2**: Controlled random search

Numerical search process involves three stochastic factors: 1) Material parameters. Material properties of the elements would be assigned through random sampling to reflect certain material parameter and its probability distribution; 2) Earthquake variability. A large number of repeated computations are done in different earthquake levels, which would be regarded as discrete random variables; 3) Concrete damage failure criterion. Nonlinear damage process will be studied based on the uncertainty of the fracture model and the constitutive model of the concrete for numerical simulation. Above all, stochastic finite element analysis is done.

Input of seismic loads: As discrete random variable, the seismic loads are input from the bottom of the bedrock ground, which is regarded as massless foundation model.

2.1.3 **Step 3**: Generalized for statistical characteristics

Based on the dynamical limit state system, failure modes of the dam shouldn't be the same because of material heterogeneity and earthquake variability, so that such work should be done to get the final failure modes, which will be provided with statistical insight, that means, studying the random process model of the progressive failure state under different dynamic conditions and analyzing the randomness and statistical rule of the progressive failure state for the dam body block.

2.2 Phases 2: Methodology for reliability analysis

The main problem for reliability analysis of the dynamical dam system, which mainly concludes five parts as follows, is the correlation between failure modes.

2.2.1 **Step 4**: Determination of limit state function

In **Step 4**, the limit state functions of the element are determined based on composite failure criterion according to different failure states (such as tension, compress, and shear) of concrete material. The composite failure criterions are as follows:

1) Maximum stress criterion

$$G_i^l = R_\mathrm{t} - \sigma_1 \tag{1}$$

where R_t is tensile strength of the dam concrete; σ_1 is the first principal stress; $G_i^l < 0$ means failure forms of elements.

2) Four parameters stress−strain relation and ruin rule

$$G_i^p = R_\mathrm{c} - (AJ_2/R + B\sqrt{J_2} + C\sigma_1 + DI_1) \tag{2}$$

where R_c is the concrete compression strength; I_1 is the first stress invariant; J_2 is the second stress invariant; $G_i^p < 0$ means failure forms of elements; A, B, C and D are defined as 2.0108, 0.9714, 9.1412 and 0.2312, respectively [15].

The traditional technique to solve Eqs. (1) and (2) is the Monte Carlo method (MCM) [16]. But running the great number of simulations required by this MCM technique can make its practical application unfeasible, and make the calculation complicated in numerical simulation and time-consuming. So, the concept of limit state surface is proposed to avoid the problem [17]. The response surface method (RSM) and its improved versions [18−22] would be employed to make the explicit expression of the limit state functions Eqs. (1) and (2), for which usually can not be expressed explicitly. This work would be done with the Latin hypercube sampling technology and the stochastic finite element calculation. So, Eqs. (1) and (2) can be expressed as Eqs. (3) and (4).

$$G_i^l(X_j) = a_i^l + \sum_{j=1}^{n} b_{ij}^l x_j + \sum_{j=1}^{n} c_{ij}^l x_j^2 \tag{3}$$

$$G_i^p(X_j) = a_i^p + \sum_{j=1}^{n} b_{ij}^p x_j + \sum_{j=1}^{n} c_{ij}^p x_j^2 \tag{4}$$

where X_j stands for the basic random variables; n is the total number of the random variables; a_i^p, a_i^l, b_{ij}^p, b_{ij}^l, c_{ij}^p and c_{ij}^l are the undetermined coefficients. Up to now, the limit state functions with explicit expression of the element are determined, which are proved to be the foundation of the failure probability calculation below.

2.2.2 **Step 5**: Reliability analysis of one element

Reliability analysis of the element under different failure criteria is the key problem of this part. The real substance of the joint failure probability of a certain element is a series system reliability problem, especially. Because the element of the structure will fail no matter which one of the failure criteria below the threshold value.

Specifically, for a set of sample value (x_1, x_1, ⋯, x_n) of the basic random variable X_j, the response sample value $G_i^p(x_j)$, $G_i^l(x_j)$ based on the response surface Eqs. (3) and (4) can be specified with the input variable. A state function whose value is only 0 or 1 is constructed as

$$I[G_i^p(x_j), G_i^l(x_j)] = \begin{cases} 1, & G_i^p(x_j) < 0 \bigcup G_i^l(x_j) < 0 \\ 0, & G_i^p(x_j) \geq 0 \bigcap G_i^l(x_j) \geq 0 \end{cases} \tag{5}$$

And so, the joint failure probability of a certain element can be calculated as

$$p_{\mathrm{f}_i} = \frac{1}{N}\sum_{j=1}^{N} I[G_i^p(x_j), G_i^l(x_j)] \tag{6}$$

where p_{f_i} means the failure probability; n is the total number of simulations; the corresponding reliability index of the element is

$$\beta_i = -\Phi^{-1}(p_{\mathrm{f}_i}) \tag{7}$$

where β_i is the reliability index; p_{f_i} is the failure probability; $\Phi^{-1}(\cdot)$ is the inverse function of normal distribution.

2.2.3 **Step 6**: Reliability analysis of one failure path

Reliability analysis of the failure path is essentially a problem of parallel structural systems consisting of the failure elements in the path. The correlation of adjacent element in the failure path would be studied in this part. According to the correlation, the probability of the representative elements in the failure path at the same time can be calculated using linearized Johnson method [23].

The basic principle of reliability index computation by linearized Johnson method is to use a single limit state surface rather than multiple limit state surfaces. The number of limit state surfaces would be gradually reduced by equivalent of the two limit state surfaces in turn until the last limit state surface, and the corresponding reliability index is the system reliability index.

Firstly, equivalent linearization function is formed as follows in the standard normal space.

$$\begin{cases} f_1 = \alpha_{11}u_1 + \beta_1 \\ f_2 = \alpha_{21}u_1 + \alpha_{22}u_2 + \beta_2 \\ \vdots \qquad\qquad \vdots \\ f_n = \alpha_{n1}u_1 + \alpha_{n2}u_2 + \cdots + \alpha_{nn}u_n + \beta_n \end{cases} \tag{8}$$

where $\sum_{j=1}^{i}\alpha_{ij}^2 = 1$, and the correlation of the limit state function can be calculated as

$$\rho_{ij} = \sum_{k=1}^{i}\alpha_{ik}\alpha_{jk} \tag{9}$$

So, the α_{ij} in Eq. (8) can be written as

$$\alpha_{ij} = \frac{\rho_{ij} - \sum_{k=1}^{j-1}\alpha_{ik}\alpha_{jk}}{\sqrt{1-\sum_{k=1}^{j-1}\alpha_{jk}^2}} \tag{10}$$

Secondly, failure boundary function between two joint elements i and j can be constructed as

$$\begin{cases} f_i = \sum_{k=1}^{n}\alpha_{ik}u_k + \beta_i = 0 \\ f_j = \sum_{k=1}^{n}\alpha_{jk}u_k + \beta_j = 0 \end{cases} \tag{11}$$

According to the reliability preserving reductions principle, failure boundary function Eq. (11) will be expressed as

$$f_E = \sum_{k=1}^{n}\alpha_{Ek}u_k + \beta_E = 0 \tag{12}$$

where α_{Ek} and β_E should satisfy the following equations

$$\begin{cases} \sum_{k=1}^{n}\alpha_{Ek}^2 = 1 \\ \beta_E = -\Phi^{-1}(\Phi(-\beta_i, \beta_j, \rho_{ij})) \end{cases} \tag{13}$$

Finally, the reliability of the failure path will be got. Compute the equivalent failure boundary of the first element and its adjacent one, then calculate the equivalent linear failure boundary of the next element. So, the failure boundary of whole system and the corresponding reliability index will be got gradually.

2.2.4 **Step 7**: Reliability analysis of system

The system of the roller compacted concrete (RCC) gravity dam is essentially a multimode relevant system as well as a series system. Based on the correlation coefficient between equivalent linear failure boundary, which comes from Eq. (9) in last step, the reliability of the system is presented through narrow interval estimation theory [24]

$$\begin{cases} P_{\mathrm{f}} \geq P_{\mathrm{f}_1} + \max[\sum_{i=2}^{k}\{P_{\mathrm{f}_i} - \sum_{j=1}^{i-1}P(E_iE_j)\}; 0] \\ P_{\mathrm{f}} \leq \sum_{i=1}^{k}P_{\mathrm{f}_i} - \sum_{i=2}^{k}\max P(E_iE_j) \end{cases} \tag{14}$$

$$\max[P(A), P(B)] \leq P(E_iE_j) \leq P(A) + P(B) \tag{15}$$

$$\begin{cases} P(A) = \Phi(-\beta_i)\Phi(-\dfrac{\beta_j - \rho_{ij}\beta_i}{\sqrt{1-\rho_{ij}^2}}) \\ P(B) = \Phi(-\beta_j)\Phi(-\dfrac{\beta_i - \rho_{ij}\beta_j}{\sqrt{1-\rho_{ij}^2}}) \end{cases} \tag{16}$$

where P_{f} means the failure probability of the system; $P(E_iE_j)$ refers to the failure probability of two paths at the same time; β_i and β_j are the reliability indices of the path i and path j, respectively; ρ_{ij} is the correlation coefficient between the two paths.

2.2.5 **Step 8**: Reliability analysis of dynamical system

Considering the randomness of earthquake, the dynamic reliability would be solved based on the full

probability formula and the numerical fitting integral method.

Horizontal seismic coefficient is an important random variable which can be written as

$$K_H=A/g \tag{17}$$

where g is the acceleration of gravity; the system reliability of gravity dam is essentially a conditional probability $P(f|A)$ under particular horizontal seismic coefficient A so that the numerical fitting integral method [25], see Eq. (18), based on the full probability formula is employed to solve the problem.

$$P_f=\int_0^a P(f|A)f(A)\mathrm{d}A \tag{18}$$

$$\beta=\Phi^{-1}(1-P_f) \tag{19}$$

where the symbol "|" represents the conditional probability; $f(A)$ is probability distribution function of the horizontal seismic coefficient A; $\Phi(\cdot)$ is the standard normal distribution function.

3 Example verification for failure modes searching

3.1 Searching process

In general, there are two ways to identify main failure mode of large engineering structure. One is from the limit state system, that means, the main failure modes are determined based on the progressive failure process in a certain limit state, which is easy to be understood and accepted by designers. The other is from the probability evaluation system, that means, the failure probability is the judgment standard, and the main failure modes are the ones which have the maximum failure probability by calculating the failure probability of all elements. But, the process of confirming failure mode from the probability evaluation system needs large amount of calculation and is not easy to reflect mechanical meaning. Therefore, the limit state system is taken for confirming the main failure modes of the gravity dam system here.

Through the limit state system, both the initial position and gradual process of the failure modes of the gravity dam is confirmed based on the nonlinear dynamic damage analysis. Considering the uncertainty of the ground motion, material property, calculation model and analysis methods, the randomness of seismic waves, dam body materials, as well as the numerical simulation method and the concrete fracture model are all studied through the numerical experiments, the research for the randomness and statistical rule of the dam concrete progressive failure process in different stress states is carried out, as a result, the influence of all sorts of randomness on structural failure paths and failure modes is revealed, and the potential failure mode is statistically confirmed.

And specifically, selecting a group of seismic waves, which have different spectrum characteristics, using different peak accelerations, ranging from 0.1g to 0.6g, and different structure models with different material parameters (random variables), also, the plasticity damage model [26−27] for concrete, smeared crack model [28], separation crack model based on XFEM [29] for simulation of the dam concrete crack expansion are employed, respectively. At the end, statistical results will be carried out for different failure modes (initial position and gradual process), and will be summarized as typical failure mode.

3.2 Verification

As one of few gravity dam which is damaged during the strong earthquake, Koyna Dam has relatively complete records and always be treated as the classical research object for dynamic damage research of concrete dams. So, the applicability of different concrete fracture models and constitutive relations, which are employed to reveal the failure modes, is verified based on such example. Calculation parameters are from Ref. [30]. The elastic modulus of dam concrete is 31.0 GPa, Poisson ratio is 0.2, density is 2643 kg/m^3, tensile strength is 2.90 MPa, fracture energy is 250 N·m, dynamic water pressure is considered according to the Westergaard formula; The seismic wave in 1967, Koyna acceleration records, is shown in Fig. 2. The calculation of Rayleigh damping factors uses the first two nature frequencies got by the linear elastic analysis.

Based on different constitutive models, the dynamic failure patterns of the Koyna Dam are revealed under the action of Koyna seismic wave through overload numerical test method, as shown in Fig. 3. At the same time, contrast diagram between the simulation results and the shaking table test [31] results are given, in which T_{Damage} means tensile damage factor.

From the above analysis, we can see that the potential failure modes are basically the same which are revealed from random numerical simulations and from the model tests and the calculated results are in good agreement with those of the actual damaged in earthquakes. This shows the different concrete fracture models and constitutive relations can simulate the damage process, and the mechanical process and significance can also be reflected so that the methodology for failure mode identification in phase 1 has the universal applicability.

4 Case study

In order to further expound the above method

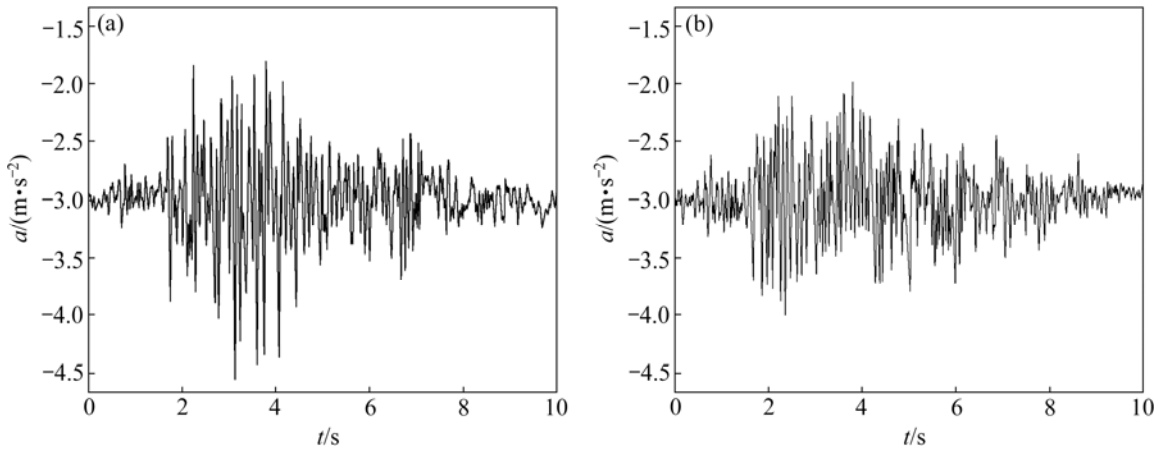

Fig. 2 Koyna acceleration records: (a) Downstream flow; (b) Vertical flow

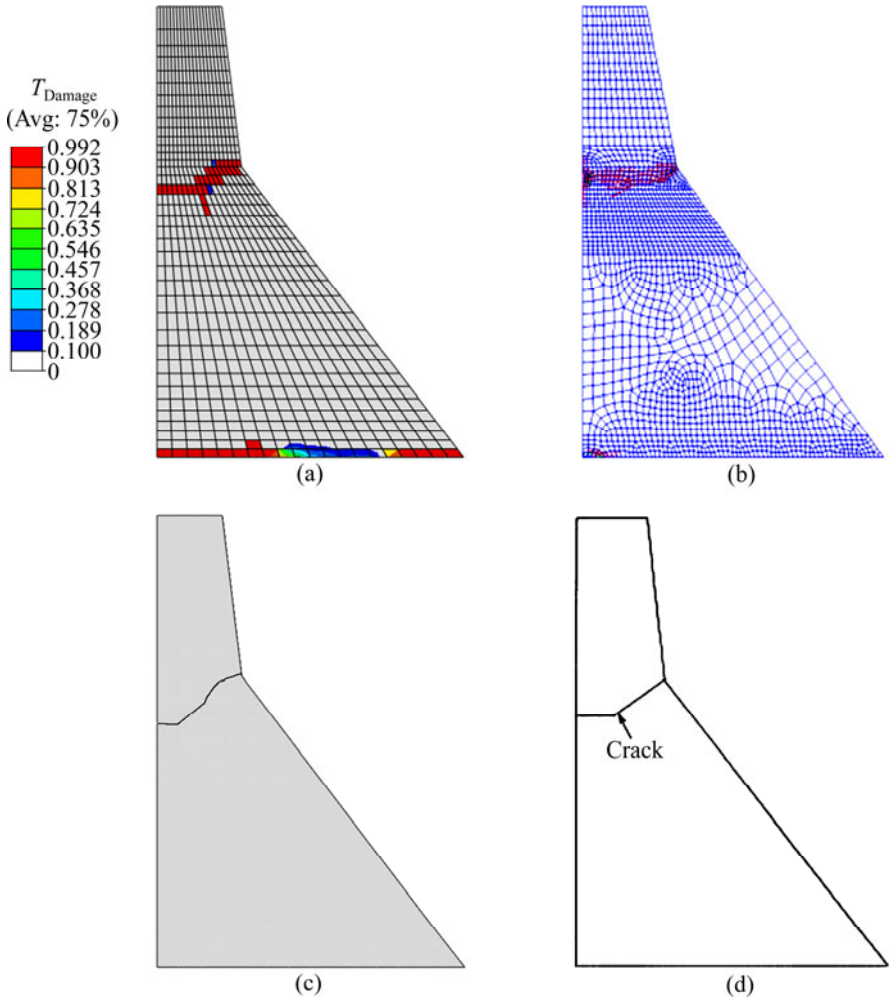

Fig. 3 Contrast diagram between simulation results and shaking table test results [31]: (a) Damaged plasticity performance; (b) Smeared cracks; (c) Discrete cracks by XFEM; (d) Shaking table test result

system in Fig. 1, we adopt a certain typical engineering project to carry out the whole calculation and analysis of the dynamic system reliability based on ABAQUS surface.

4.1 Description of typical dam

One RCC gravity dam, of which the height is 149 m, is studied. The design earthquake intensity is VIII degree. The horizontal peak acceleration is 0.284*g* with the exceedance probability of 2% per 100 a. Figure 4 gives the dam section and the finite elements. In the seismic analysis, dam foundation will be regarded as massless foundation, of which the dynamic elastic modulus is 16.5 GPa, Poisson ratio is 0.25. Westergaard formula

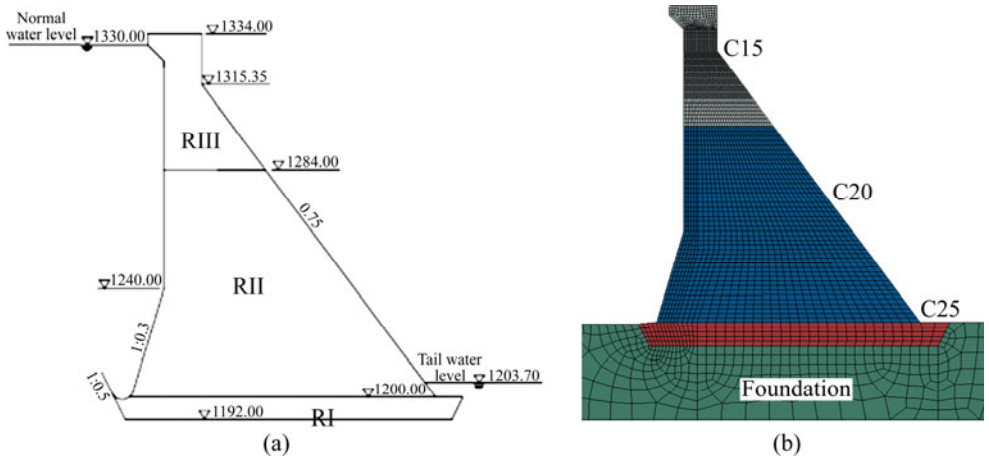

Fig. 4 Dam section and finite elements (Unit: m): (a) Dam section; (b) Finite element modal (2D)

will be adopted to calculate the hydrodynamic pressure. The load combination is water pressure (both the upstream and the downstream), dam body mass, upstream silt pressure, uplift pressure at the foundation surface and the seismic loads. The material parameters of the dam are regarded as the random variables while other variables which variation coefficient is less than 0.05 will be regarded as deterministic ones. Especially, the earthquake will be regarded as discrete random variable. The selection of the parameters is according to the geological exploration data, the original design research report and "The water conservancy and hydropower engineering structure reliability design code" (GB50199—1994), as listed in Table 1. A dynamic magnification factor of 1.3 is considered for the tensile strength and the dynamic modulus of elasticity based on the static ones.

Table 1 Statistical characteristics of random variables

Type	Variable	Distribution pattern	Mean value	Coefficient of variation
Dam	Elasticity modulus of C25/GPa	Normal	43.8	0.10
	Elasticity modulus of C20/GPa	Normal	37.8	0.10
	Elasticity modulus of C15/GPa	Normal	29.0	0.10
Foundation	Elasticity modulus/GPa	Normal	18.0	0.10
	Cohesion/MPa	Normal	1.50	0.20
	Friction factor	Lognormal	1.20	0.15
Layers of dam	Friction factor	Lognormal	0.91	0.15
	Cohesion/MPa	Normal	1.13	0.20
Foundation base	Friction factor	Lognormal	1.05	0.15
	Cohesion/MPa	Normal	1.05	0.20

4.2 Analysis of model and variables

1) Basic material variables

The basic material variables are listed in Table 1.

2) Earthquake load

Due to the strong uncertainty and randomness of the ground motion, it needs to select the seismic waves reasonably to ensure the numerical results. At present, in the seismic design for dam, we mainly adopt the actual and artificial earthquake ground-motion histories. Here, the Koyna wave, Chi-Chi wave, Loam-Prieta wave, Northridge wave and the artificial one corresponding to the code response spectrum are selected to consider the influence of seismic amplitude and frequency characteristics.

The normalized actual earthquake records and artificial ones are shown in Figs. 5(a)−(e). By adjusting the characteristic of the frequency spectrum of seismic waves, the seismic response spectrum parameters are similar to that of the design code. The adjusted characteristic of the frequency spectrum of the seismic response spectrum curves is shown in Fig. 5(f). The effect of two-dimension is considered in the load cases combination with both the horizontal and vertical waves, and the vertical acceleration amplitude is 2/3 of the horizontal one.

4.3 Searching process of failure modes

First of all, according to the concrete physical and mechanical parameters of probability statistics model (see Table 1), assign the material characteristic to the element through random sampling, in order to reflect its spatial distribution. We considered five groups of material parameter samples, with five groups of different seismic waves in Fig. 5, and six different acceleration amplitudes (Peak ground acceleration, A_{GA}=0.284g, 0.399g, 0.426g, 0.483g, 0.586g and 0.710g), respectively. We adopt different concrete damage models to research

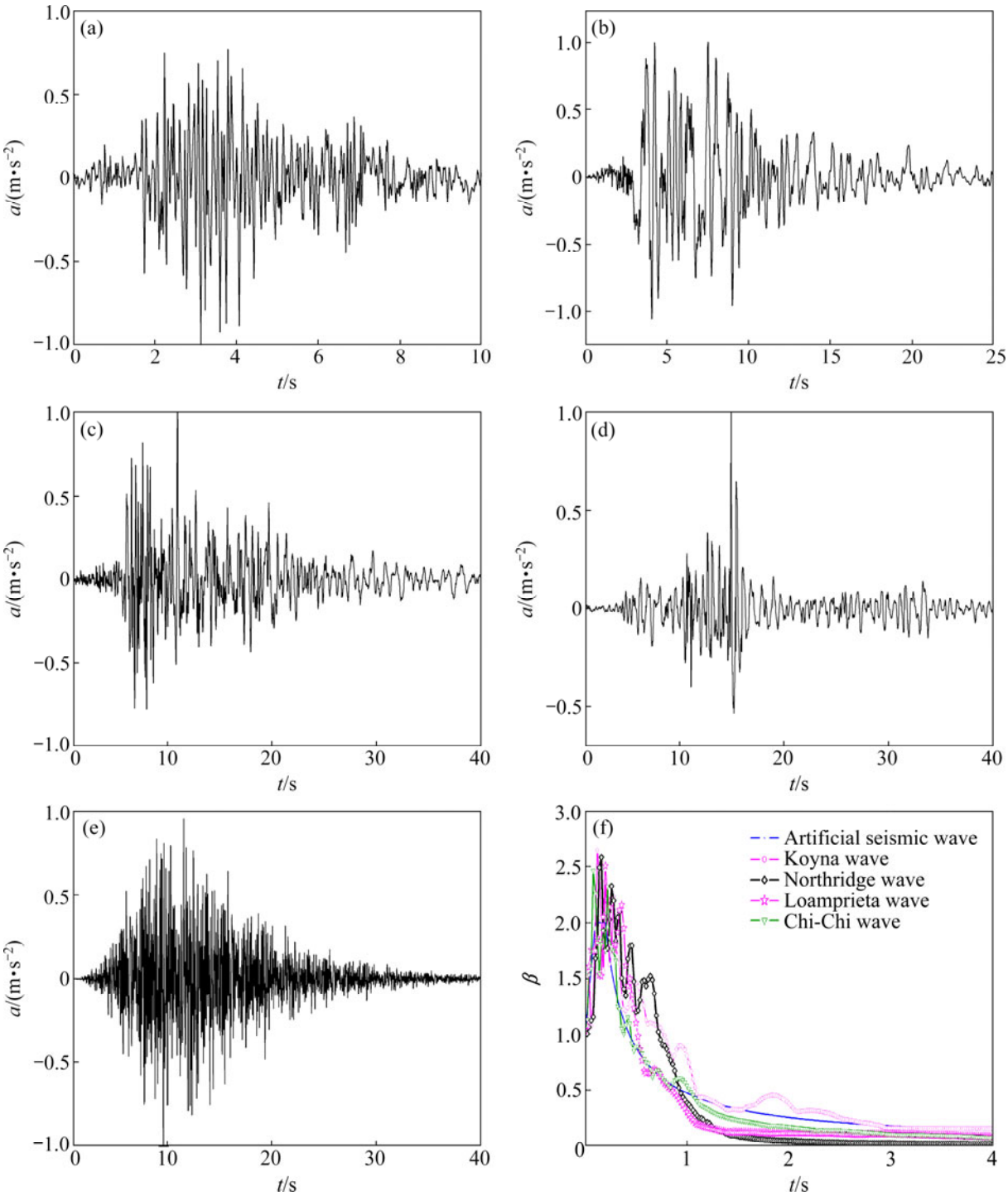

Fig. 5 Normalized seismic waves and response spectrum curves: (a) Koyna wave; (b) Northbridge wave; (c) Loam-Prieta wave; (d) Chi-Chi wave; (e) Artificial wave; (f) Response spectrum curves

the structure of dynamic failure mechanism, as shown in Figs. 6−8, a total of 150 calculations are made. What need to explain is, for A_{PG}=0.284g, no damaged situation of the structure appears so that no damaged pattern is given.

In Fig. 6, through the concrete plastic damage model simulation, the typical dam body structure dynamic failure damage distribution patterns are got. Figure 7 shows the results through the smeared crack model simulation, and Fig. 8 shows the results through the Separation crack model simulation.

4.4 Generalization and verification for failure mode

The statistical analysis for 150 groups of different failure modes under different earthquake loads are given in Table 2.

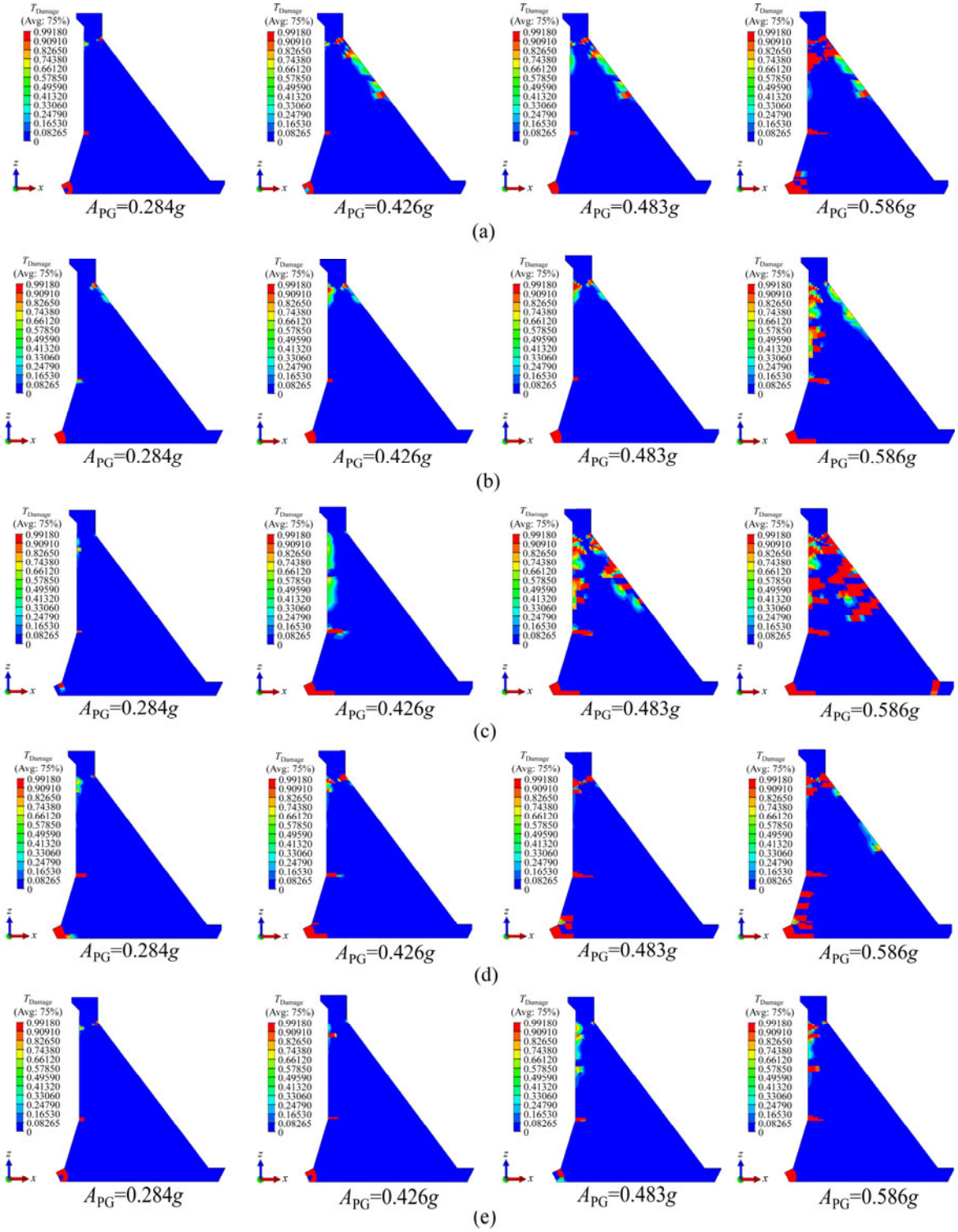

Fig. 6 Dynamic damage modes for four PGAs under plastic damage constitutive modal: (a) Dynamical failure modes under Koyna waves; (b) Dynamical failure modes under Chi-Chi waves; (c) Dynamical failure modes under Loam-Prieta waves; (d) Dynamical failure modes under Northridge waves; (e) Dynamical failure modes under artificial waves

For heterogeneous material dam under the action of earthquake in the different level, the dam failure pattern is not the same. Through statistics, it can be thought that the potential failure modes mainly contain the following five kinds (shown in Fig. 9) in the strong earthquakes: 1) Cracks expanding from the dam heel along the foundation surface to the dam toe; 2) Expanding from the upstream folding slope to the dam internal, probably it can develop into a penetrating crack in the dam; 3) Expanding from the downstream of different concrete zoning to the dam internal; 4) Expanding from the upstream of different concrete zonings to the dam internal,

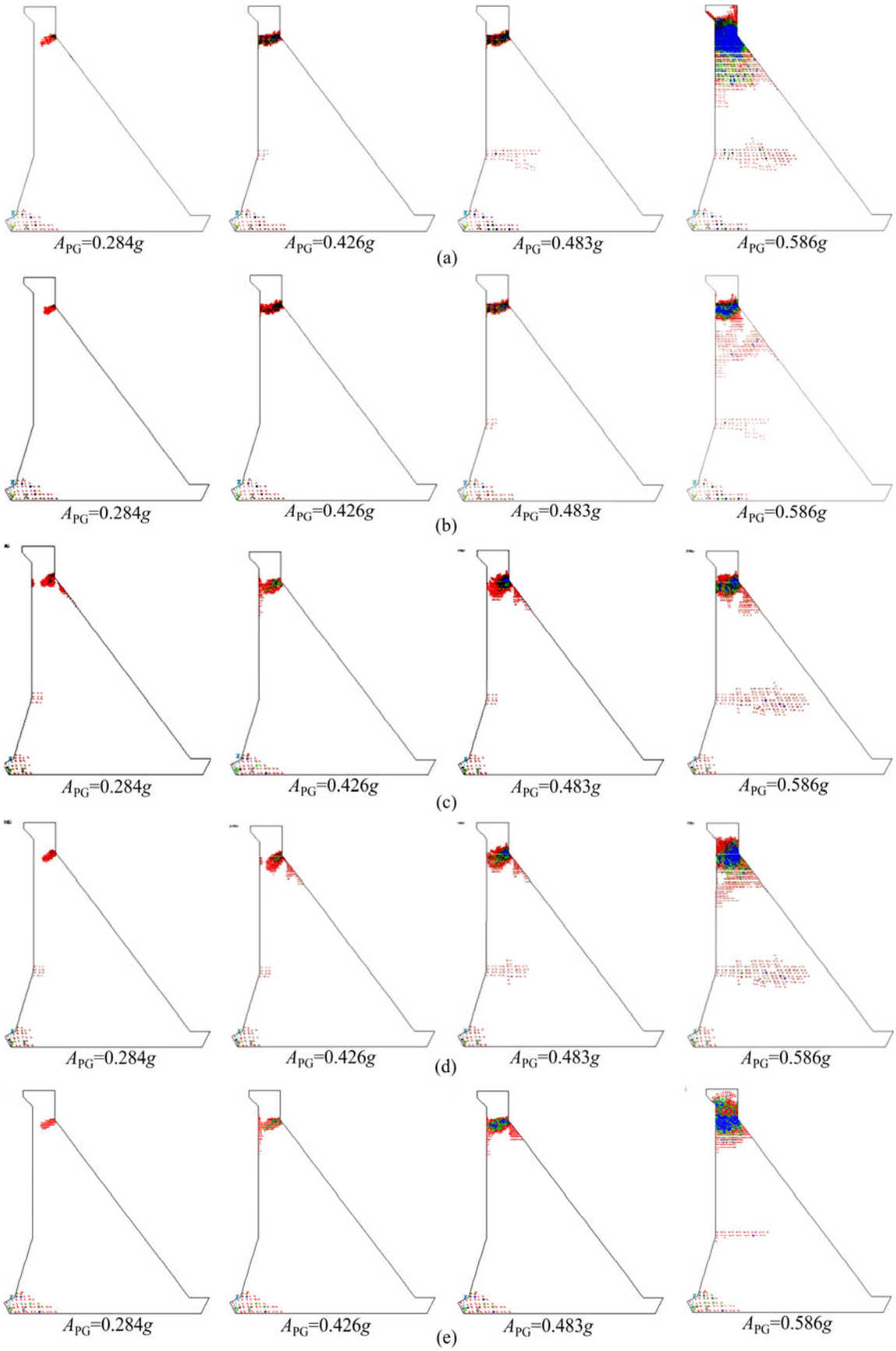

Fig. 7 Dynamic damage modes for four PGAs under smeared crack model: (a) Dynamical failure modes under Koyna waves; (b) Dynamical failure modes under Chi-Chi waves; (c) Dynamical failure modes under Loam-Prieta waves; (d) Dynamical failure modes under Northridge waves; (e) Dynamical failure modes under artificial waves

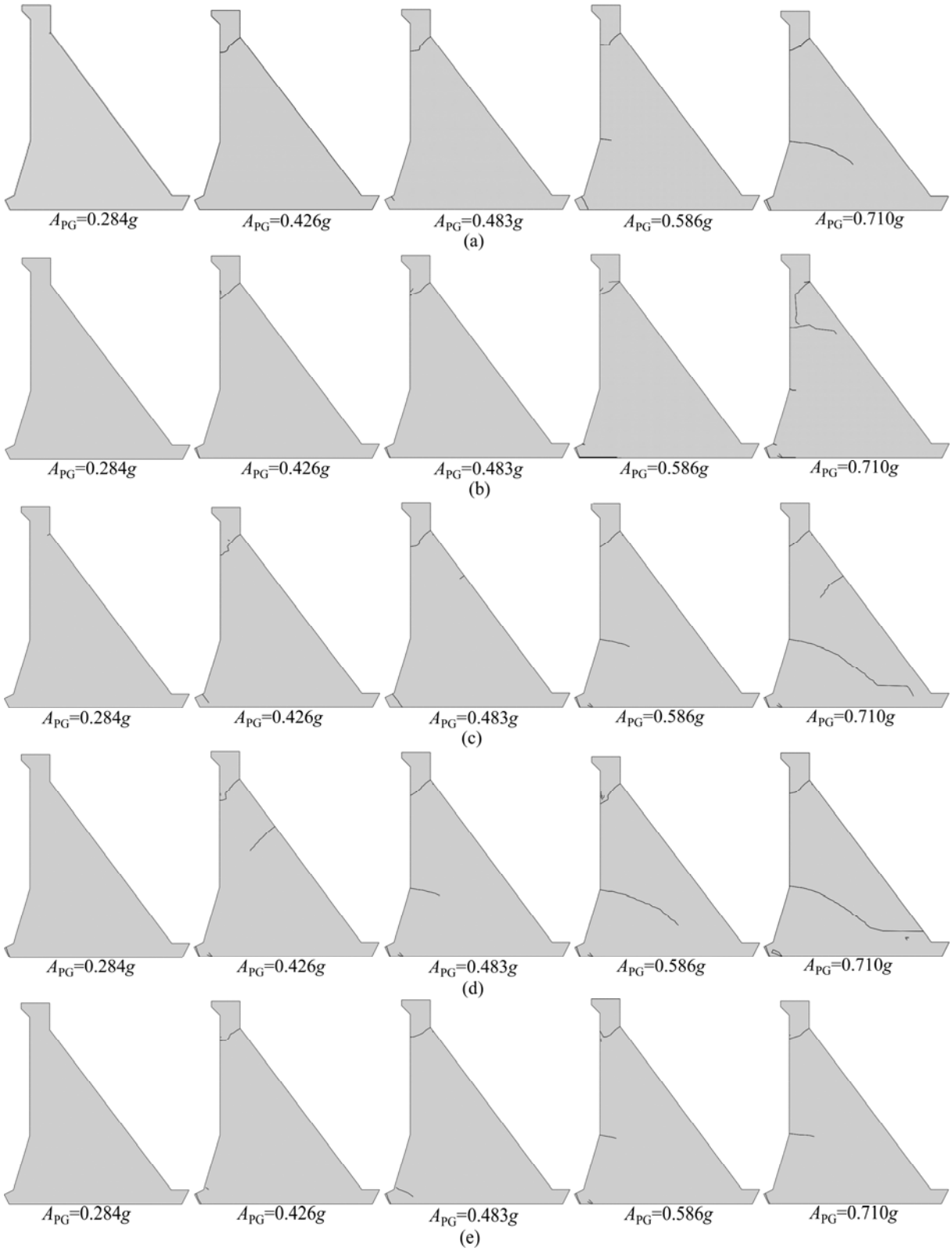

Fig. 8 Dynamic damage modes for five PGAs under separation crack model based on XFEM: (a) Dynamical failure modes under Koyna waves; (b) Dynamical failure modes under chi-chi waves; (c) Dynamical failure modes under Loam-Prieta waves; (d) Dynamical failure modes under Northridge waves; (e) Dynamical failure modes under artificial waves

probably it can develop into penetrating cracks through upstream to downstream; 5) Expanding from downstream folding slope along about 45° inclined plane to the dam internal, possibility developing into a penetrating crack till the upstream face. According to the potential failure mode and progressive failure process of

the gravity dam, it can be generalized out the power system failure paths with the starting point and the development path, as shown in Fig. 10.

Table 2 Different failure mode statistics under different seismic loads

Typical failure mode	Load				
	0.284*g*	0.426*g*	0.483*g*	0.586*g*	0.710*g*
Mode 5	13/150	139/150	142/150	142/150	136/150
Mode 4	0/150	3/150	13/150	28/150	64/150
Mode 3	0/150	13/150	7/150	17/150	73/150
Mode 2	0/150	3/150	37/150	115/150	137/150
Mode 1	7/150	23/150	117/150	123/150	146/150

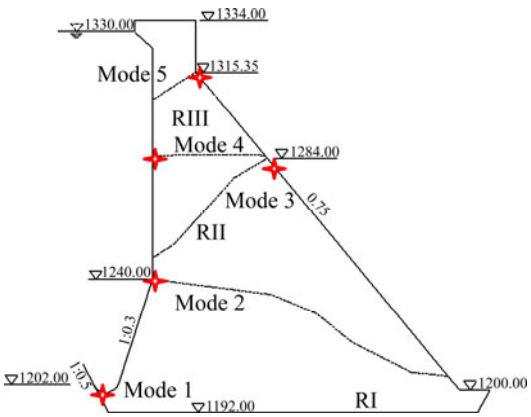

Fig. 9 Potential failure modes under earthquake loading (Unit: m)

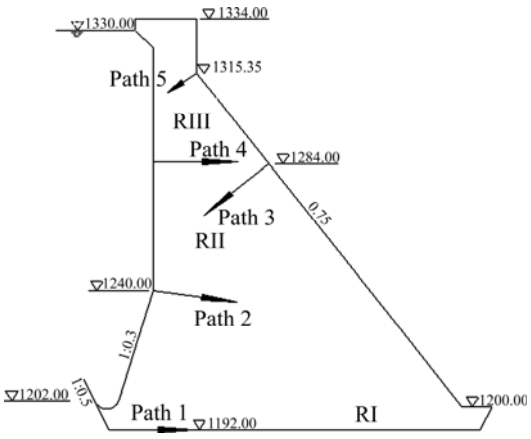

Fig. 10 Generalization for failure paths (Unit: m)

4.5 Reliability analysis of one element

For example, at A_{PG}=0.2*g*, random variables in Table 1 are sampled and combined through the method and technology in Refs. [32−33], and then the limit state function value of the element 1 in Fig. 11 is got through the deterministic finite element method, also, the response surface equation is got based on the coupling Monte-Carlo and response surface method (MC-RSM). That is, through the linear regression method, the coefficients in each response surface functions (Eqs. (3) and (4)) are determined, so that the explicit expression can be written as

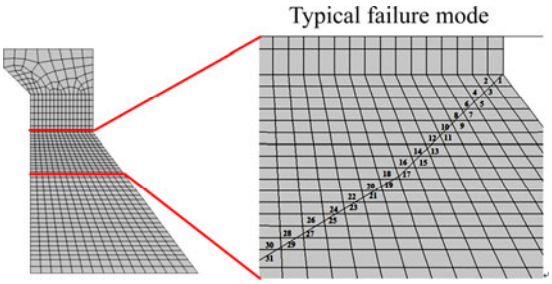

Fig.11 Failure process and probability of typical mode

$$\begin{aligned} G = {} & 8.0315\times10^{6} + 4.242\times10^{5}\times f_1(E_{15}) - \\ & 3.505\times10^{5}\times f_2(E_{20}) - 1.074\times10^{5}\times f_3(E_{25}) - \\ & 9.976\times f_4(E_{\text{base}}) + 6.885\times10^{6}\times f_5(R_3) + \\ & 2.205\times10^{5}\times f_6(E_{\text{base}}^2) + 1.072\times10^{5}\times f_7(E_{20}^2) + \\ & 5.489\times10^{4}\times f_8(E_{15},E_{20}) - 1.082\times10^{5}\times \\ & f_9(E_{15},E_{\text{base}}) - 1.927\times10^{5}\times f_{10}(E_{\text{base}},E_{20}) \end{aligned} \quad (20)$$

where subfunctions in Eq. (20) are expressed in Table 3.

Table 3 Subfunctions in response surface equation of first element of failure mode 5 under A_{PG}=0.2*g*

Subfunction	Equation
$f_1(E_{15})$	$1.482\times10^{-10}\times E_{15}-4.298$
$f_2(E_{20})$	$1.137\times10^{-10}\times E_{20}-4.298$
$f_3(E_{35})$	$9.814\times10^{-11}\times E_{25}-4.298$
$f_4(E_{\text{base}})$	$2.388\times10^{-10}\times E_{\text{base}}-4.298$
$f_5(R_5)$	$1.457\times10^{-7}\times R_3-2.996$
$f_6(E_{\text{base}}^2)$	$[f_4(E_{\text{base}})]^2$
$f_7(E_{20}^2)$	$[f_2(E_{20})]^2$
$f_8(E_{15}, E_{20})$	$f_1(E_{15})\times f_2(E_{20})$
$f_9(E_{15}, E_{\text{base}})$	$f_1(E_{15})\times f_4(E_{\text{base}})$
$f_{10}(E_{\text{base}}, E_{20})$	$f_2(E_{20})\times f_4(E_{\text{base}})$

Furthermore, 100000 times stochastic simulations are done on the response surface so that the failure probability is got, that is 99.399%, and the corresponding reliability index is −2.512. According to the method above, all of the failure probabilities and its corresponding reliability indexes in the failure mode 5 listed in Fig. 11 are obtained, and at the same time, the correlation coefficients of the different elements are listed in Table 4.

4.6 Reliability analysis of one path

Under A_{PG}=0.2*g*, the correlation coefficients between elements in the failure mode 5 in Table 4 are considered, then the linearized Johnson method expressed in Eqs. (8)−(13) is employed to calculate the failure probability of the path. In this process, we

Table 4 Correlation coefficients between elements in failure mode 5 under A_{PG}=0.2g

Element No.	1	2	3	4	5	6	7
1	1.00	0.989	0.993	0.982	0.985	0.974	0.977
2	0.989	1.00	0.921	0.918	0.973	0.996	0.997
3	0.993	0.921	1.00	0.996	0.988	0.982	0.994
4	0.982	0.918	0.996	1.00	0.995	0.996	0.999
5	0.985	0.973	0.988	0.995	1.00	0.998	0.998
6	0.974	0.996	0.982	0.996	0.998	1.00	0.997
7	0.977	0.997	0.994	0.999	0.998	0.997	1.00

calculate all of the failure probability of the modes (modes 1−5). The reliability indexes respectively are 8.620, 8.280, 5.326, 5.312 and 4.604, also, the corresponding failure probabilities are 6.418×10^{-17}, 6.260×10^{-16}, 5.458×10^{-8}, 5.884×10^{-8} and 2.114×10^{-6}. In the same way, reliability indexes of the potential instability models under other horizontal ground motions are listed in Table 5.

Table 5 Reliability indexes of failure modes under different horizontal seismic coefficients

Horizontal seismic coefficient A	Mode 1	Mode 2	Mode 3	Mode 4	Mode 5
0 (*)	9.105	11.138	12.254	13.679	14.664
0.1	8.885	10.813	10.134	11.228	11.364
0.2	8.620	8.280	5.326	5.312	4.604
0.3	8.531	6.134	4.323	3.492	2.386
0.4	8.168	5.120	3.524	2.613	−0.543
0.5	8.026	3.812	1.672	2.377	−2.142

*—Horizontal seismic coefficient 0 is static condition.

4.7 Reliability analysis of system

Gravity dam reliability belongs to a system reliability problem, first of all, sliding correlation between different failure modes are analyzed, then the Ditlevsen narrow limit formula estimating system failure probability of the up and down limit.

For example, Correlation coefficients between that 5 potentialpaths are analyzed when the horizontal seismic coefficient 0.2 (A_{PG}=0.2g) and the results are listed in Table 6, the system failure probability is about 0.000211%−0.000212% (corresponding reliability index is about 4.604) by using the Ditlevsen approximate formula. Similarly, the condition probability of the system and its corresponding reliability index of the dam are calculated respectively in different horizontal seismic coefficients with the results given in Table 7. Furthermore, logarithmic form of the condition probabilities was described because it presents numerically small.

Table 6 Correlation coefficients between paths under A_{PG}= 0.2g

Mode	1	2	3	4	5
1	1.000	−0.117	−0.121	−0.124	−0.143
2	−0.117	1.000	0.942	0.791	0.816
3	−0.121	0.942	1.000	0.882	0.903
4	−0.124	0.791	0.882	1.000	0.931
5	−0.143	0.816	0.903	0.931	1.000

Table 7 System reliability calculations under earthquakes

Horizontal seismic coefficient A	Upper control limit(*) of probability, $P(f/A)$	lg[$P(f/A)$]	Reliability index, β
0.00	2.4665×10^{-18}	−17.6079	9.105
0.10	1.0842×10^{-17}	−16.9649	8.885
0.15	5.5761×10^{-10}	−9.2536	6.137
0.20	2.1138×10^{-6}	−5.6749	4.604
0.25	1.7849×10^{-5}	−4.7484	4.135
0.30	8.5164×10^{-3}	−2.0697	2.386
0.35	0.0819	−1.0867	1.392
0.40	0.7064	−0.1509	−0.543
0.45	0.9102	−0.0409	−1.342
0.50	0.9839	−0.0071	−2.142

*—Upper limit value will be used because failure probability limit is very narrow.

The upper limit value of the failure probability in Table 7 with the horizontal seismic coefficients will be used to fit a curve (as shown in Fig. 12), to get the fitting relationship between the stability system failure probability of the whole dam and the horizontal seismic coefficients, with is expressed as

$$\begin{cases} P_{\mathrm{f}}(A)=8.37\times10^{-17}A+2.46\times10^{-17}, & 0<A<0.1 \\ P_{\mathrm{f}}(A)=10^{C+B_1A+B_2A^2+B_3A^3+B_4A^4}, & 0.1<A<0.5 \end{cases} \tag{21}$$

where C=−49.5954, B_1=503.4886, B_2=−2150.1072, B_3=4269.2127, B_4=−3175.2234. The goodness of fit between A=0−0.5 is 0.9937, which is very close to 1.0.

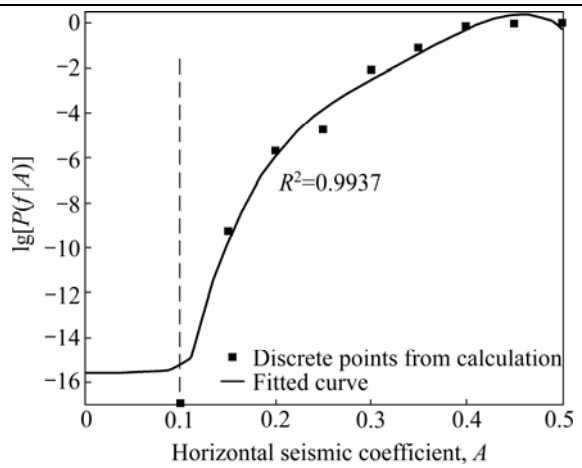

Fig. 12 Fitted curve between failure probability and horizontal seismic coefficient

4.8 Reliability analysis of dynamical system

According to Ref. [34], the PDF of the horizontal earthquake acceleration coefficient obeys the following distribution:

$$f(A) = Bb\mathrm{e}^{-bA},\ A \geq 0 \tag{22}$$

where both B and b are coefficients, and here B=0.0499, b=19.948 according to Ref. [25].

Finally, the dam failure probability of the dynamical system is P_f=3.87155×10^{-5} according to Eqs. (21)−(22) as well as Eqs. (18)−(19) by definite integral calculation from A=0 to A=0.5, and the corresponding reliability index is 3.952.

When the horizontal seismic coefficient is 0, the failure probability of the dam is P_f=2.4665×10^{-18}; and the corresponding reliability index is about 9.105. In contrast, under the dynamic condition, the failure probability has a dramatic increase to P_f=3.8715×10^{-5}. So, the dynamic effects on the stability of the dam structure seem significant, and specifically, the failure modes 3, 4 and 5 near the dam crest are the keys to the dam safety based on risk analysis methodologies.

5 Conclusions

1) The structure system reliability analysis based on the paths (or modes) according to the engineering experience is not accurate so that a new method to search the failure modes on the limit state system based on numerical tests is studied and the failure probability calculation method of the system including three levels is deduced.

2) Considering the randomness of spectrum characteristics and peak acceleration of seismic waves as well as material parameters of the dam, potential sliding paths of the dam subjected to earthquake can be identified by generalized statistics.

3) Based on SFEM, the limit state function of dynamic sliding is built according to rigid limit state criteria and response surface method (RSM) under certain seismic loading, and the reliability index is got as well. Then, considering the coherence between different failure paths, the reliability index of the system can be estimated by Ditlevsen narrow-bound method. Finally, the stochastic of seismic load is taken into account, the numerical integration method based on complete probability formula is used to get the dynamic system reliability.

4) For the next work, the random seismic waves should be better considered and generated, and the damage process and failure modes of concrete gravity dams affected by uncertain material properties and ground motion input should be studied by numerical simulation with the influences of concrete heterogeneity taken into account in the further study.

Acknowledgement

The authors would like to thank Tianjian University of Civil Engineering and the Foundation for Innovative Research Groups of the National Natural Science Foundation of China (51021004), and we appreciate the supports from the State Key Laboratory of Hydraulic Engineering Simulation and Safety (Tianjin University). The authors also wish to thank the respected reviews of this work, whose comments significantly improved the clarity and content of this work.

References

[1] ZHU Jun-song, ZI Jin-jia, LIU Xia. A reliability analysis of antiskid stability between the layers of dengke RCC gravity dam [J]. China Rural Water and Hydropower, 2011(1): 115−118.

[2] FAN Shu-li, CHEN Jian-yun, FAN Wu-qiang, LI Jing. Reliability analysis of roller compacted concrete gravity dams subjected to earthquake [J]. Chinese Journal of Rock Mechanics and Engineering, 2008, 3(3): 564−571.

[3] XU Qiang, CHEN Jian-yun, LI Jing. Calculation method for system reliability of dam based on Bayes theory [J]. Journal of Dalian University of Technology, 2011(1): 84−89.

[4] ZHONG H, LIN G, LI X Y, LI J. Seismic failure modeling of concrete dams considering heterogeneity of concrete [J]. Soil Dynamics and Earthquake Engineering, 2011, 31: 1678−1689.

[5] WU Qing-xi, ZHUO Jia-shou. Dynamic reliability analysis of gravity dams using a second-order sequence response surface method [J]. Journal of Vibration Engineering, 2001, 14(2): 224−227.

[6] JIA Chao, ZHANG Qi-hai. Research of the safety effects of level weak plane on RCC gravity dams [J]. Water Power, 2007, 33(9): 23−25.

[7] XU Qiang, CHEN Jian-yun, LI Jing. Concrete gravity dam reliability analysis on tension failure path under non-stationary ground motion processes [J]. Engineering Mechanics, 2011, 28(3): 123−128.

[8] XU Qiang, LI Jing, CHEN Jian-yun. Concrete gravity dam reliability analysis on tension failure path under non-stationary ground motion processes [J]. Engineering Mechanics, 2011, 28(3): 123−128.

[9] ALONSO E. Risk analysis of slopes and its application to slopes in

Canadian sensitive clays [J]. Geotechnique, 1976, 26(3): 453−472.

[10] TANG W H, YÜCEMEN M S, ANG A H S. Probability based short term design of slopes [J]. Can Geotech J, 1976, 13(3): 201−215.

[11] CHRISTIAN J T, LADD C C, BAECHER G B. Reliability applied to slope stability analysis [J]. Geotech Eng Div – ASCE, 1994, 120(12): 2180−2207.

[12] GRIFFITHS D V, FENTON G A. Influence of soil strength spatial variability on the stability of an undrained clay slope by finite elements [C]// Slope Stability 2000, Proceedings of GeoDenver 2000. Denvor, USA: 2000: 184−193.

[13] HUSEIN A I, HASSAN W F, ABDULLA F A. Uncertainty and reliability analysis applied to slope stability [J]. Structural Safety, 2000, 22: 161−187.

[14] ALTAREJOS-GARCÍA L, ESCUDER-BUENO I, SERRANO-LOMBILLD A. Methodology for estimating the probability of failure by sliding in concrete gravity dams in the context of risk analysis [J] Structural Safety, 2012, 36: 1−13.

[15] XIONG Tie-hua, CHANG Xiao-lin. Application of 3-D stochastic FEM based on response surface in large structure reliability analysis [J]. Journal of Wuhan University of Hydraulic and Electric Engineering, 2005, 38(1): 125−128.

[16] XU B, LOW B K. Probabilistic stability analysis of embankments based on finite element method [J]. Geotech Geoenviron Eng, 2006, 132(11): 1444−1454.

[17] SMITH M. Influence of uncertainty in the stability analysis of a dam foundation. [J]. Dam Maint Rehabil 2003: 151−158.

[18] BUCHER C G, BOURGUND U. A fast and efficient response surface approach for structural reliability problems [J]. Structural Safety, 1990, 7: 57−66.

[19] RAJASHEKHAR M R, ELLINGWOOD B R. A new look at the response surface approach for reliability [J]. Structural Safety, 1993, 12(3): 205−220.

[20] LIU Y W, FRED MOSES. A sequential response surface method and its application in the reliability analysis of aircraft structural systems [J]. Structural Safety, 1994, 16: 39−46.

[21] LIU Ji, LI Yun. An improved adaptive response surface method for structural reliability analysis [J]. Journal of Central South University, 2012, 19(4): 1148−1154.

[22] KIM S H, NA W S. Response surface method using vector projected sampling points [J]. Structural Safety, 1997, 19(1): 3−19.

[23] LIU Ning, LI Tong-chun, ZHUO Jia-shou. A method for searching the most possible failure mode by on 3-D SFEM [J]. Journal of Hydraulic Engineering, 1996(3): 36−43.

[24] DITLEVSEN O. Narrow reliability bounds for structural system [J]. Strut Mech, 1979, 4(1): 117−122.

[25] JIA Chao, LIU Ning, CHEN Jin. Slope risk analysis under the earthquake effect [J]. Chinese Journal of Rock Mechanics and Engineering, 2005, 24(04): 703−707.

[26] LEE J, FENVES G L. A plastic-damage concrete model for earthquake analysis of dams [J]. Earthquake Engineering and Structural Dynamics, 1998: 937−956.

[27] ABAQUS, Inc.ABAQUS/Standard user's manual [M]. Version 6.10. Providence, RI, 2010.

[28] CERVERA M, OLIVER J, FARIA R. Seismic evaluation of concrete dam via continuum damage Model [J]. Earthquake Engineering and Structural Dynamic, 1995, 24(9): 1225−1245.

[29] MOËS N, BELYTSCHKO T. Extended finite element method for cohesive crack growth [J]. Engineering Fracture Mechanics, 2002(69): 813−833.

[30] CHOPRA A K, CHAKRABARTI P. The Koyna earthquake and the damage to Koyna dam [J]. Bull Seism Soc Am, 1973, 63(2): 381−397.

[31] HALL J F. The dynamic and earthquake behavior of concrete dams: Review of experimental behavior and observational evidence [J]. Soil Dyn Earthquake Eng, 1988, 7: 58−121.

[32] FARAVELLI L. A response-surface approach for reliability analysis [J]. Eng Mech, ASCE, 1989, 15(12): 2763−2781

[33] BUEHER C G, BOURGUND U. A fast and efficient response surface approach for structural reliability problems [J]. Structural Safety, 1990, 7(1): 57−66.

[34] Earth Scientific Consultants Mecann W Associates. Seismic hazard map for Puerto Rico 1994 [R]. Puerto Rico Report Prepared for Seismic Safety Commission Puerto Rico 1994.

(Edited by DENG Lü-xiang)